Article

DIAGNOSTIC SUPPORT OF SKIN LESION CLASSIFICATION USING CNN AND SOFT ATTENTION

Khoi Do Hoang[2,†,] [ID] [*]

1   Lecturer: Viet Dung Nguyen; dung.nguyenviet1@hust.edu.vn

2   Author: Khoi Do Hoang; khoi.dh200332@sis.hust.edu.vn

*   Correspondence: khoido8899@gmail.com; Tel.: +84-9360-192-58

†   Current address: 1st Dai Co Viet Street, Ha Noi, Viet Nam

Abstract: Today, the rapid development of industrial zones leads to an increased incidence of skin diseases because of polluted air. According to a report by the American Cancer Society, it is estimated that in 2022 there will be about 100,000 people suffering from skin cancer and more than 7600 of these people will not survive. In the context that doctors at provincial hospitals and health facilities are overloaded, doctors at lower levels lack experience and having a tool to support doctors in the process of diagnosing skin diseases quickly and accurately is essential. Along with the strong development of artificial intelligence technologies, many solutions and tools to support the diagnosis of skin diseases have been researched and developed. These include DenseNet, InceptionNet, ResNet, NasNet, SeNet, EfficientNet, VGGNet. In this study, another approach to building tools to aid in the diagnosis of skin pathologies is proposed. SOTA (state of the art) models DenseNet, InceptionNet, ResNet, NasNet, MobileNet combined with Soft-Attention are used as backbone. In addition, personal information such as age and gender are also used. In addition, a new loss function that takes into account the imbalance of the data is also proposed. Experimental results on data set HAM10000 show that using InceptionResNetV2 with Soft-Attention and new loss function gives 90 percent accuracy, mean of precision, f1-score, recall-score, and AUC scores of 0.81, 0.81, 0.82, and 0.989, respectively, are improvements compared to published indexes. Besides, using MobileNetV3Large combined with Soft-Attention and new loss function, even though the number of parameters is 11 times less, the number of floors is 4 times less, it achieves 86 percent accuracy and 30 times faster diagnosis.

Keywords: AI Diagnosis, Skin Sancer, Skin Lesion Classification, Deep Learning, Machine Learning)

1. Introduction

1.1. Problem Statement

Skin cancer is one of the most common cancers leading to worldwide death. Every day, more than 9500[14] people in the United States are diagnosed with skin cancer. Otherwise, 3.6[14] million people are diagnosed with basal cell skin cancer each year. According to the Skin Cancer Foundation, the global incidence of skin cancer continues to increase[13]. In 2019, it is estimated that 192,310 cases of melanoma will be diagnosed in the United States[13]. On the other hand, if patients are early diagnosed, the survival rate is correlated with 99 percent. However, once the disease progresses beyond the skin, survival is poor[13]. Moreover, with the increasing incidence of skin cancers, low awareness among a growing population, and a lack of adequate clinical expertise and services, there is a need for effective solution.

Recently, deep learning particularly, and machine learning in general algorithms have emerged to achieve excellent performance on various tasks, especially in skin disease diagnosis tasks. AI-enabled computer-aided diagnostics (CAD) has solutions in three main categories: Diagnosis, Prognosis, and Medical Treatment. Medical imaging, including ultrasound, computed tomography, magnetic resonance imaging, and X-ray image is used extensively in clinical practice. In Diagnosis, Artificial Intelligence (AI) algorithms are

applied for disease detection to save progress execution before these diagnosis results are considered by a doctor. In Prognosis, AI algorithms are used to predict the survival rate of a patient based on his/her history and medical data. In Medical Treatment, AI models are applied to build solutions to a specific disease, medicine revolution is an example. In various studies, AI algorithms have provided various end-to-end solutions to the detection of abnormalities such as breast cancer, brain tumors, lung cancer, esophageal cancer, skin lesions, and foot ulcers across multiple image modalities of medical imaging[13].

In order to adapt the rise in skin cancer case, AI algorithms over the last decade has a great performance. Some typical models that can be mentioned are DenseNet[17], EfficientNet[20], Inception[19], MobileNets[20][21][22], ResNet[23][24], and NasNet[33]. Some of these models which have been used as a backbone model in this paper will be discussed in the Related Work section.

1.2. Related Works

Skin lesion classification is not a new area, since there are many great performance models constructed. One of the most cutting-edge technologies that have been used is Soft-Attention as stated in[14]. Soumyyak et al construct several models formed by the combination of a backbone model including DenseNet201[17], InceptionResNetV2[19], ResNet50[23][24], VGG16[25] and Soft-Attention layer. Using those above backbones has been tried by many previous papers. Rishu Garg et al [3] uses transfer learning approach with CNN based model. Amirreaza et al [5] do not only use those above backbone model but also used InceptionV3[19] model. Another paper that uses the backbone models is [9], Hemanth et al decide to use EfficientNet[18] and SeNET[35] instead and CutOut[36] method which involves creating holes of different sizes on the images i.e. technically making a random portion of image inactive during data augmentation process. [12] also used Deep Convolution Neural Network, Peng Yao et al used RandArgument which crops an image into several images from a fixed size, DropBlock which is used for regularization, Multi-Weighted New Loss which is used for dealing with the imbalanced data problem, end-to-end Cumulative Learning Strategy which can more effectively balance representation learning and classifier learning without additional computational cost. Another state of the art is GradCam and Kernel SHAP[6], Kyle Young et al create model agnostic, local interpretable methods that can highlight pixels that the trained network deems relevant for the final classification.

Otherwise, there are also many state of the art whose great performance on skin lesion classification. The Student and Teacher Model is also a high performance model in 2021[2], which is created by Xiaohan Xing et al as the combination of two model which share the memory with each other. Therefore, they can take full advantage of what others learn. SkinLinkNet[15] and WonderM[16] are both tested the effect of segmentation on skin lesion classification problem created by Amirreza et al and Yeong Chan et al, respectively. In WonderM, the method used is padding the image so that the image has the shape increased from (450,600) to (600, 600). In SkinLinkNet, instead resize the image down to (448, 448). Both of SkinLinkNet and WonderM use UNet to do the segmentation task, though they use EfficientNetB0 and DenseNet to do the classification task, respectively. Another approach is using metadata including gender, age, and capturing position as stated in [10] by Nil Gessert et al.

On the other hand, skin lesion classification problems are not only applied by Deep Learning but also Machine Learning. Random Forest, XGBoost, and Support Vector Machines are tested by [3] of Rishu Garg et al. Besides, Isolation Forest is applied before the soft-max activation of the deep learning model to detect out of distribution skin lesion images as stated in[5] by Amirreza Rezvantalab et al. Matrix Transformation, besides is also applied before the soft-max activation function in [8] by Michele Alberti et al.

Work	Approach
[14]	Combination of Backbone Model and Soft Attention. Backbone model includes DenseNet201, InceptionResNetV2, VGG16, ResNet50, ResNet34
[3]	Transfer Learning with CNN based model
[5]	Transfer Learning with CNN based model including DenseNet201, InceptionResNetV2, VGG16, ResNet50, ResNet34, and InceptionNetV3
[9]	Transfer Learning with CNN based model including EfficientNet and SeNet. Data augmentation process used CutOut to create random sized hole considered as an inactive portion of image.
[12]	Transfer Learning with CNN based model. Data augmentation process uses RandArgument to split picture into several pictures which is used to train. DropBlock and Multi-Weight Loss Function are used to deal with the imbalanced.
[6]	GradCam and Kernel SHAP, two model agnostic, local interpretable methods that can highlight pixels that the trained network deems relevant for the final classification.
[2]	Student and Teacher Model is the combination of two model which share the memory learned with others.
[15]	SkinLinkNet uses the image whose shape is (448,488) for training. Unet and EfficientNetB0 are used for segmentation and classification task respectively.
[16]	WonderM uses the image whose shape is (600,600) created by padding for training. Unet and DenseNet are used for segmentation and classification task respectively.
[10]	MetaData including age, gender, and capture position are used to gain higher performance of the model. The models used in this paper are CNN-based model
[3]	Traditional Machine Learning Algorithms are applied including Random Forest, XGBoost, and Support Vector Machine
[5]	Matrix Factorization are applied before the softmax activation function
[8]	Isolation Forest are applied distribution skin lesion images before fedding into the softmax activation function.
[5]	Matrix Factorization are applied before the softmax activation function.

Table 1. Related Works Summary. This table is a summary of the approach to skin lesion classification and segmentation. The first column illustrate the cite to the paper research. Column 2 shows a brief summary of the method that is stated in the associated paper.

1.3. Objectives

In this paper, the effect of metadata on classifying skin disease will be analyzed. On the other hand, by analyzing the combination of several backbone models, I will also construct an optimized model that has the ability to classify in a balanced way between classes instead of well identifying the majority of classes.

2. Materials and Methods

2.1. Data

2.1.1. Image Data

The data set used in this paper is the HAM10000 data set published by Havard University Dataverse[7]. There are total 7 classes in this data set containing Actinic keratoses and intraepithelial carcinoma or Bowen's disease (AKIEC), Basal cell Carcinoma (BCC), benign keratosis-like lesions (solar lentigines / seborrheic keratoses andchen-planus like keratoses, BKL), dermatofibroma (DF), melanoma (MEL), melanocytic nevi (NV), and vascular lesions (angiomas, angiokeratomas, pyogenic granulomas and hemorrhage, VASC). The distribution of the data set is shown in the table below:

Class	AKIEC	BCC	BKL	DF	MEL	NV	VASC	Total
No. Sample	327	514	1099	115	1113	6705	142	10015

Table 2. Data Distribution in HAM10000. This table illustrate the distribution of all class in the data set. The detail name of the skin disease in the data set can be found at the Abbreviations
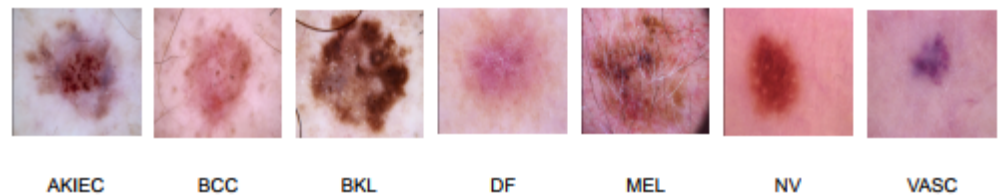

Figure 1. Example image of each class

More than 50 percent of lesions are confirmed through histopathology (HISTO), the ground truth for the rest of the cases is either follow-up examination (FOLLOWUP), expert consensus (CONSENSUS), or confirmation by in-vivo confocal microscopy (CONFOCAL). On the other hand, before being used for training the whole data is shuffled then split into two part. 90 percent and 10 percent of the data is used for training and validating respectively.

In the previous research[14], the image data is augmented for all class, the number of image increase to 18015 images. Since, this data is imbalanced, using augmented data may cause the problem of well classify on the classes almostly taking the number of samples. In this paper, instead of augmenting data, metadata is used. The way of processing metadata is discussed in MetaData section. Images in this data set has the type of RGB and shape of (450, 600). However, Each backbone need the different input size of image as well as the range of pixel value. DenseNet201[17] require the input pixels values are scaled between 0 and 1 and each channel is normalized with respect to the ImageNet data set. In Resnet50 and Resnet152[23][24], the images are converted from RGB to BGR, then each color channel is zero-centered with respect to the ImageNet data set, without scaling. InceptionResNetV2[18], on the other hand, will scale input pixels between -1 and 1. Similarly, three versions of MobileNet[20][21][22], NasNetMobile and NasNetLarge[33] require the input pixel is in range of -1 and 1.

2.1.2. Metadata

The HAM10000 data set[7] also contain the metadata of patient including gender, age, and the capturing position as well as the test data set containing 857 images. During the data exploration term, the age category miss 57 data points, which is decided to remove this 57 samples. In the gender and capturing position category contain some samples of unknown. Instead of removing, these "unknowns" data points is kept and considered as "prefer not to say". Besides, the label of the whole data is preprocessed into one-hot vector.

2.2. Model Schema

2.2.1. Input Schema

Using metadata as another input is not new. In paper[10], they decide to keep the missing value and set its value to 0. The sex and anatomical site are categorical encoded. The age, on the other hand is numerical normalized. After processing, the metadata is fed into a two-layer neural network with 256 neurons each. Each layer contains batch normalization, a ReLU[34] activation, and dropout with $p = 0.4$. The network's output is concatenated with the CNN's feature vector after global average pooling. Especially, they use a simply data augmentation strategy to address the problem of missing values in metadata. During training, they randomly encode each property as missing with a probability of $p = 0.1$.

In this paper, the unknowns is kept as a type as discussed in Metadata section. Sex, anatomical site and age are also category encoded and numerical normalized, respectively. After processing, the metadata is then concatenated and fed into a dense layer of 4096 neurons. Finally, this this dense layer is then concatenate with the output of Soft-Attention which is then discussed in Soft-Attention section. The Input schema is described as follow:
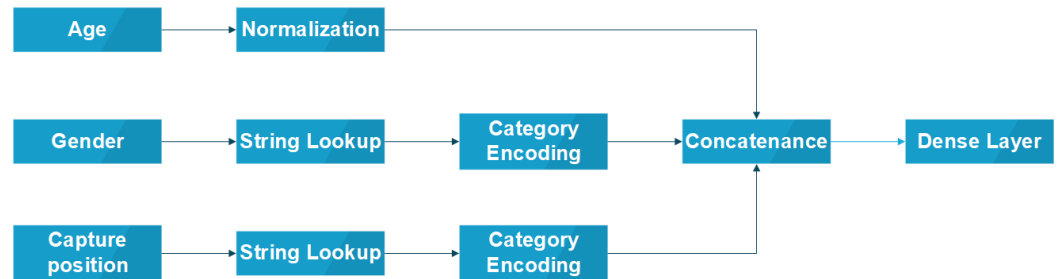

Figure 2. Input Schema

2.2.2. Soft-Attention

Applying the Soft-Attention layer in deep learning is not a new approach. Soft-Attention has been used in various applications: image caption generation in [28] and handwriting verification in [29] respectively. In skin lesion classification, Soft-Attention is used to increase the performance of the model as described in [14]. Soft-Attention can ignore irrelevant areas of the image by multiplying the corresponding feature maps with low weights. The function below describes the flow of the Soft-Attention module:

$$f_{sa} = \gamma t \sum_{k=1}^{K} softmax(W_k * t)$$

In order to apply Soft-Attention, there are two main steps. Firstly, the input tensor is put in grid-based feature extraction from the high-resolution image, where each grid cell is analyzed in the whole slide to generate a feature map[30]. This feature map called $t \in R^{h \times w \times d}$ where $h, w,$ and d is the shape of tensor generated by a Convolution Neural Network(CNN), is then input to a 3D convolution layer whose weights is $W_k \in R^{h \times w \times d \times K}$. The output of this convolution is normalized using the softmax function to generate K = 16 attention maps. These 16 attention maps are aggregated to produce a weight function called α. This α function is then multiplied with feature tensor t and scaled by γ, a learnable scalar. Finally, the output of Soft-Attention function f_{sa} is the concatenation of the beginning feature tensor t and the scaled attention maps.
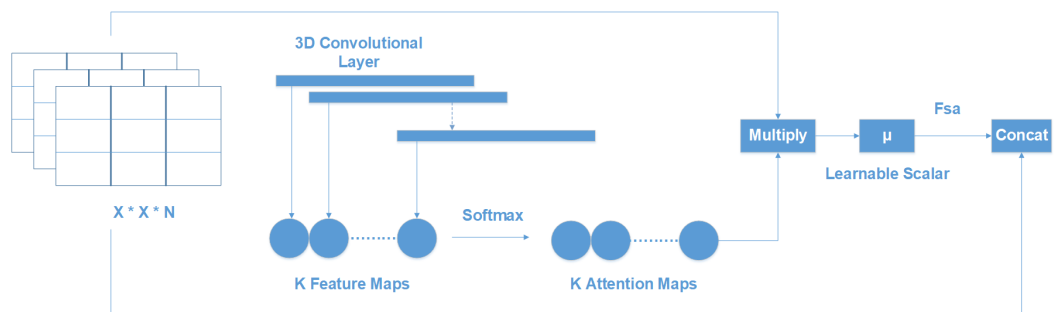

Figure 3. Soft-Attention Module

In this paper, the Soft-Attention layer is applied in the same way in this paper[14]. The Soft-Attention module is described in the following diagram:
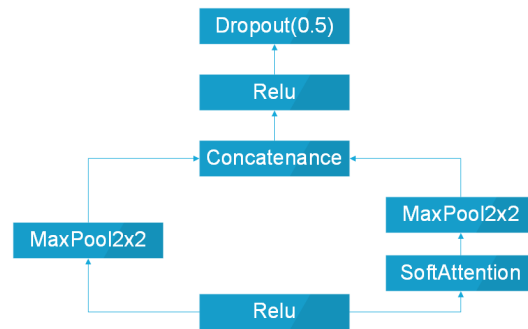
Figure 4. Soft-Attention Module

After feeding into ReLU function layer, the feature map is processed in two paths. The first path is the 2-dimensional Max Pooling. In the second path, the feature map, on the other hand is fed into the Soft-Attention Layer before the 2-dimensional Max Pooling. After all, these two paths are then concatenated, fed into a ReLU layer, and a Dropout with the probability of 0.5.

2.2.3. Backbone Model Architecture

In this paper, the backbone models used in this paper are DenseNet201[17], Inception[19], MobileNets[20][21][22], ResNet[23][24], and NasNet[33]. The combination of DenseNet201, InceptionResNetV2 and Soft-Attention layer are both tested by the previous paper[14] with a great performance. Otherwise, Resnet50 also well classify but with much less number of parameter and depth than based on its f1-score and precision stated. Therefore, in this paper, the performance of the model Resnet152 and NasnetLarge which has the larger number of parameter and depth is analyzed. On the other hand, three version of MobileNet and the NasnetMobile will also be analyzed which has a small number of parameter and depth.

Model	Size(MB)	Parameters	Depth
Resnet50	98	25.6M	107
Resnet152	232	60.4M	311
DenseNet201	80	20.2M	402
InceptionResNetV2[37]	215	55.9M	449
MobileNet	16	4.3M	55
MobileNetV2	14	3.5M	105
MobileNetV3Small	Unknown	2.5M	88
MobileNetV3Large	Unknown	5.5M	118
NasnetMobile	23	5.3M	308
NasnetLarge	343	88.9M	533

Table 3. Size and Parameters and Depth of backbone model used in this paper. This table summarizes the properties of the backbone models. The size column illustrates how many space need to store the model in megabyte. The parameters column demonstrate the number of parameters in the associated model. The last column, depth show the number of hidden layers in that model. Parameters and Depth are two crucial element to evaluate the optimized model stated in the Objective section.

2.2.4. Model

The whole architecture of the model used for image feature extraction is applied in the same way in paper [14]. Metadata branch, otherwise is preprocessed before feeding into a dense layer then concatenate with the output of Soft-Attention layer. It is described in the figure below:
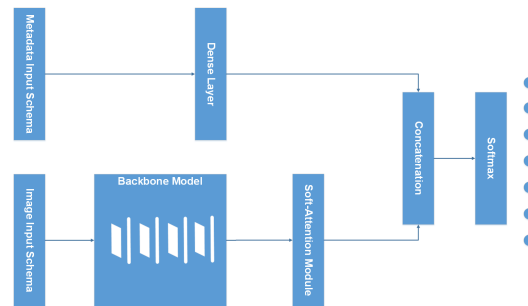
Figure 5. Overall Mobile-based Model Architecture

The figure 6 illustrates the overall structures of the combination of backbone models and Soft-Attention, which is used in this research. In detailed the combination of DenseNet201 and Soft-Attention is formed by replacing the three last DenseBlock, Global Average Pooling, and the fully-connected layer with the Soft-Attention Module. Similarity, ResNet50 and ResNet152 is also replaced the three last Residual Block, Global Average Pooling, and the fully connected layer with the Soft-Attention module. InceptionResNetV2, on the other hand, is replaced the Average Pool and the last Dropout with the Soft-Attention Module. Besides, the two last Normal Cell in NasNetLarge is replaced with the Soft-Attention module.
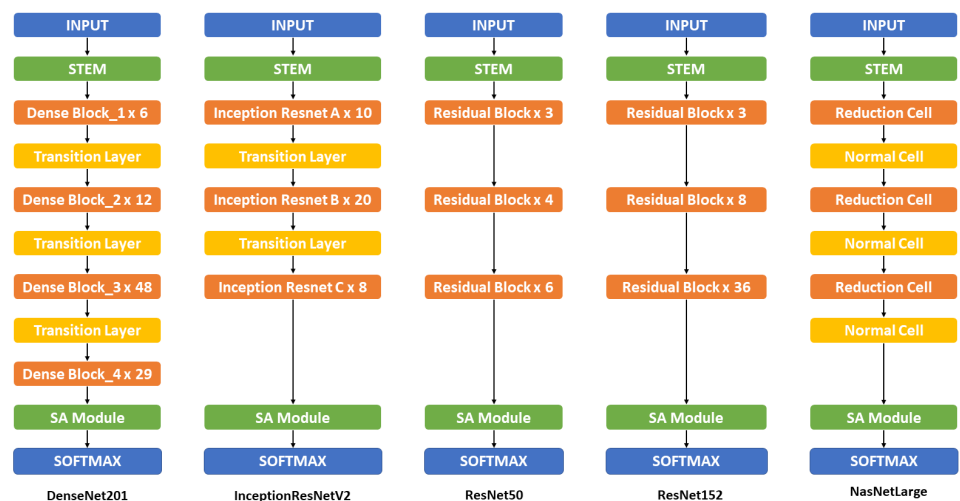

Figure 6. Overall Model Architecture. This figure show the overall structure of the backbone model (non mobile-based model) including DenseNet201, InceptionResNetV2, ResNet50, ResNet152, and NasNetLarge. The detail structure and information can be found at the Apendix A

The figure 7, on the other hand shows the detailed structure of mobile-based mobile and its combination with Soft-Attention. All of the MobileNet versions combine with the Soft-Attention module by replacing the two last convolution 1x1 by Soft-Attention module. The NasNetMobile, otherwise, combine with the Soft-Attention module by replacing the last Normal Cell.
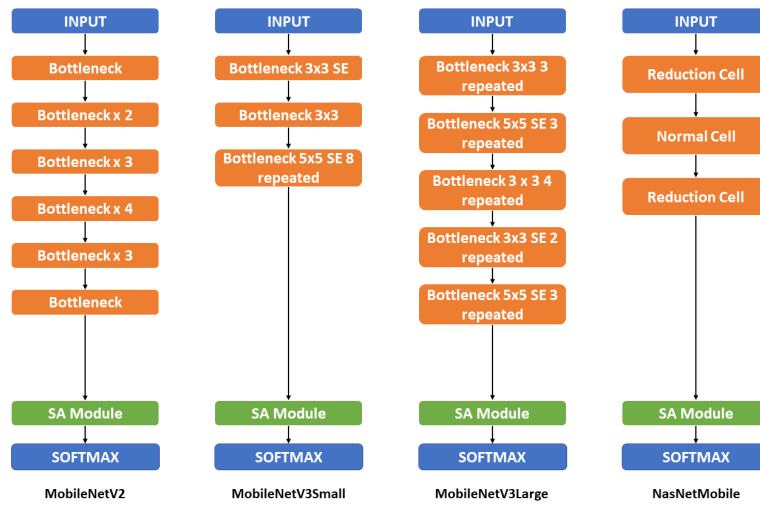
Figure 7. Overall Mobile-based Model Architecture. This figure show the overall structure of the mobile-based backbone model including MobileNetV2, MobileNetV3Small, MobileNetV3Large, and NasNetMobile. The detail structure and information can be found at the Apendix B

2.3. Loss Function

The loss function used in this paper is categorical cross-entropy. Consider $X = [x_1, x_2, \ldots, x_n]$ as the input feature, $\theta = [\theta_1, \theta_2, \ldots, \theta_n]$. Let N, and C is the number of training examples and number of class respectively. The categorical cross-entropy loss is presented as:

$$L(\theta, x_n) = -\frac{1}{N} \sum_{c=1}^{C} \sum_{n=1}^{N} W_c \times y_n^c \times \log(\hat{y}_n^c)$$

where $\hat{y}_i^c$ is the output of model and y_i^c is the target that the model should return, W_c is the weight of class c. Since the data set face the imbalanced problem then I applied the class weight for the loss. This formula below is used to calculate the class weight:

$$W = N \odot D$$

$$D = \begin{bmatrix} \frac{1}{C \times N_1} & \frac{1}{C \times N_2} & \cdots & \frac{1}{C \times N_n} \end{bmatrix} = \frac{1}{C} \odot \begin{bmatrix} \frac{1}{N_1} & \frac{1}{N_2} & \cdots & \frac{1}{N_n} \end{bmatrix}$$

where N is the number of training sample, C is the number of class, N_i is the number of sample in each class i. D is the matrix contain the inverse of $C \times N_i$.
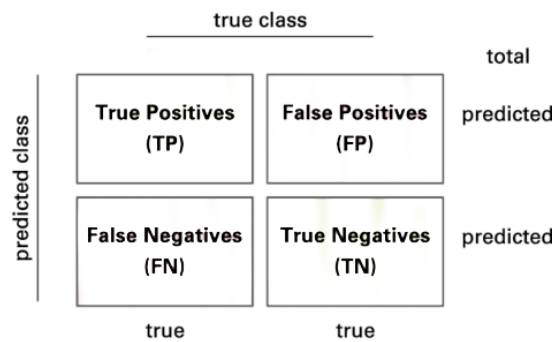
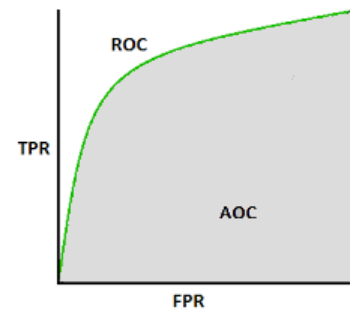*2.4. Evaluation Metrics*

Figure 8. Confusion Matrix

Figure 9. Area Under the Curve

In this paper, the model is evaluated by using the confusion matrix and related metrics. The figure 4 illustrates the presentation of a 2×2 confusion matrix used for 2 class. Consider

a confusion matrix A with C number of class. Let A^i and A^j is the set of A rows and columns respectively.

$$A = \begin{bmatrix} a_{11} & a_{12} & \dots & a_{1j} \\ a_{21} & a_{22} & \dots & a_{2j} \\ \vdots & \vdots & & \vdots \\ a_{i1} & a_{i2} & \dots & a_{ij} \end{bmatrix}$$

The True Positive(TP) of all class in this case is the main diagonal of the matrix A. The following method are used to calculate the False Positives(FP), False Negatives(FN), and True Negatives(TN) of all class:

$$FP = -TP + \sum_{k=1}^{i} A_k^i \qquad FN = -TP + \sum_{k=1}^{j} A_k^j$$

$$TN_c = \sum_{i=1}^{C}\sum_{j=1}^{C} a_{ij} - \left[\sum_{k=1}^{i} A_{i=ck}^i + \sum_{k=1}^{j} A_{j=ck}^j \right] + a_{i=cj=c} \implies TN = \begin{bmatrix} TN_1 & TN_2 & \dots & TN_c \end{bmatrix}$$

Then, the model is evaluated by the following metrics:

$$\text{Sensitivity(Sens)} = \frac{TP}{TP + FN} \qquad \text{Specificity(Spec)} = \frac{TN}{TN + FP}$$

$$\text{Precision} = \frac{TP}{TP + FP} \qquad \text{F1 Score} = \frac{2 \times TP}{2 \times TP + FP + FN + TN}$$

$$\text{Accuracy} = \frac{TP + TN}{TP + FP + FN + TN} \qquad \text{Balanced Accuracy} = \frac{\text{Sens} + \text{Spec}}{2}$$

The last metric is the AUC score standing for Area Under the Curve which is the Receiver Operating Curve(ROC) that indicate the probability of TP versus the probability of FP.

2.5. Traning

Before training, the data set is split into three sub datasets including training, validation, and testing. In this paper, the graphic card that is used to train is Nvidia RTX TitanV. In order to make the comparison fair, all the model in this paper is trained with Adam Optimizer[27]. The initial learning rate is set to 0.001, an learning rate reduction schedule is setup with the minimum learning rate is 0.0000001 with the factor of 0.2, the epsilon argument of the optimizer is set to 0.1. On the other hand, Early Stopping is also set up, if the accuracy of validation set does not increase after 25 epochs, the training will stop.

3. Results

The accuracy of all model is presented in the figure below:

InceptionResNetV2	DenseNet201	ResNet50	VGG16
0.79	0.84	0.76	0.77

Table 4. Accuracy of the model with augmented data

InceptionResNetV2	DenseNet201	ResNet50	Resnet152	MobileNetV2
0.89	0.89	0.70	0.57	0.81

MobileNetV3Large	MobileNetV3Small	NasNetLarge	NasNetMobile
0.84	0.78	0.86	0.86

Table 5. Accuracy of the model with metadata

According to the Table 4 and 5, it is clear that the model trained with metadata has a higher accuracy than the model trained with augmented data only. While Inception-ResNetV2 and DenseNet201 trained with augmented data have accuracy of 0.79 and 0.84 respectively, their training with metadata has both the accuracy of 0.89. Furthermore, Resnet50 trained with augmented data has the accuracy that outperform the Resnet50 and is twice as high as Resnet152 trained with metadata. On the other hand, mobile model including MobileNetV2, MobileNetV3Large, and NasNetMobile, even though has a much smaller number of parameters and depth than the other model, they have a quite good accuracy of 0.81, 0.84, 0.86, respectively.

Moreover, the model trained with augmented data does not only have low accuracy but their f1-score and the recall score also are imbalanced according to figure 10. As a results, augmented data model does not classify well on all class as InceptionResNetV2 trained on augmented data have f1-score on class df and akiec is just above 0.3 and 0.4, separately while InceptionResNetV2 trained on metadata and the new weight loss can classify well in a balanced way arcoding to the figure 11. However, only DenseNet201, InceptionResNetV2, and NasNetLarge whose depth are equal or larger than 400 have balanced f1-score on class. The others still face the imbalanced term. Since this data set is not balanced, therefore using augmented data can make the model more bias to the class which has larger sample. Using the metadata, though still make the model bias, it does contributes to the improvement of the performance of the model.

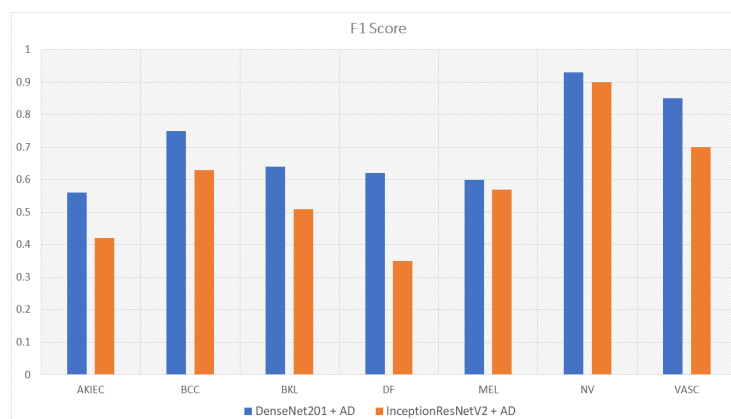**Figure 10.** F1 Score on each class of each model. The class contain AKIEC, BCC, BKL, DF, MEL, NV, VASC which is denoted in the abbreviation section. The models showed in the above bar chart include DenseNet201 and InceoptionResNetV2 which are the two best model after hyper tuning. AD means the two models are trained with augmented data created during the training, there is neither no metadata nor weight loss contribution.

Figure 11. The f1-score on each class of two models: DenseNet201 and InceptionResNetV2 which are trained with the MetaData (MD) and the Weight Loss (WL) function. In this case, there is no contribution from the augmented data.The detail architecture of the model can be seen at the appendix section A. The f1-score performance results of other models can be seen at appendix section C.1

This problem is also true with the recall score according to table 7. DenseNet201, InceptionResNetV2, trained with augmented data has expected value of recall of 0.56, 0.69, respectively, while the combination of DenseNet201, Metadata and the new weight loss function achieve the expected value of recall: 0.82. Therefore, metadata does improve the model performance by reducing the amount of data needed for achieving higher results. On the other hand, the reason why the model become much more balanced is the weighted loss function. Weight loss function has ability to solve the imbalanced class samples by adding a weight related to the number of samples in each class. DenseNet201, InceptionResNetV2 trained with the new weighted loss function have recall in akiec of 0.85. 0.82, respectively, as opposed to their training in akiec without weighted loss function: 0.65 and 0.37.
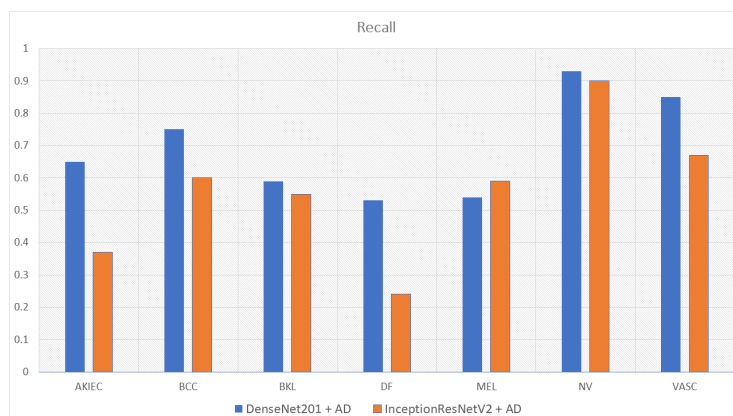
Figure 12. Recall score on each class of each model. The class contain AKIEC, BCC, BKL, DF, MEL, NV, VASC which is denoted in the abbreviation section. The models showed in the above bar chart include DenseNet201 and InceoptionResNetV2 which are the two best model after hyper tuning. AD means the two models are trained with augmented data created during the training, there is neither 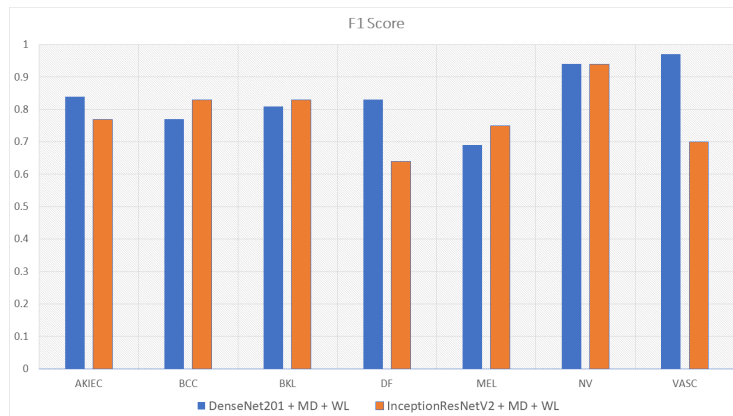no metadata nor weight loss contribution. The detail architecture of the model can be seen at the appendix section A. The f1-score performance results of other models can be seen at appendix section C.2

Figure 13. The recall score on each class of two models: DenseNet201 and InceptionResNetV2 which are trained with the MetaData (MD) and the Weight Loss (WL) function. In this case, there is no contribution from the augmented data.The detail architecture of the model can be seen at the appendix section A. The f1-score performance results of other models can be seen at appendix section C.2
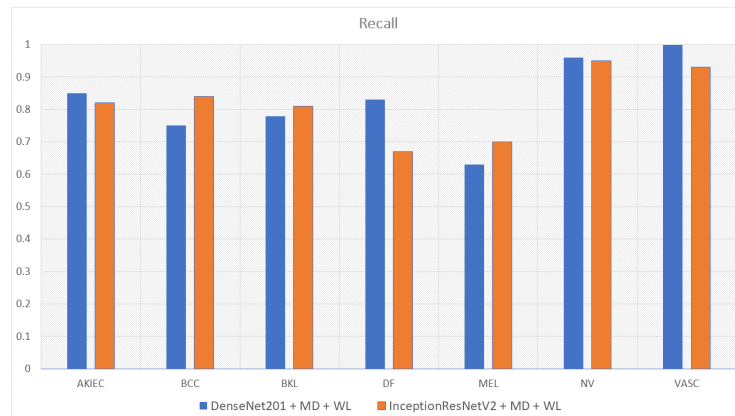
Another interesting point found during the experiment is that MobileNetV2, MobileNetV3 and NasNetMobile have small number of parameters and depth, though have relative good performance. MobileV3large, MobileV3Small, NasNetLarge and NasNetMobile outperform others on classifying class df with the recall score of 0.92, 1, 0.92, 0.92, separately according to the table A4 appendix C.2. It's transparent that MobileNetV3Large and NasNetMobile are the two best performance model. Nevertheless, MobileNetV3Large has less number of parameters and depth than NasNetMobile.

Model	MobileNetV3Large	DenseNet201	InceptionResnetV2
No. Parameters	**5.5M**	20.2M	55.9M
Depth	**118**	402	449
Accuracy	0.86	0.89	0.90
Time Prediction(s/epochs)	**116**	1000	3500

Table 6. How Performance of MobileNetV3Large be optimized

The table 9 shows that the MobileNetV3Large, though the number of parameters are much smaller than the DenseNet201, InceptionResNetV2, achieve the accuracy nearly to the others. In detail, MobileNetV3Large whose the number of parameters is 5.5 millions which is four and ten times less than DenseNet201 and InceptionResNetV2, respectively. The depth of MobileNetV3Large, on the other hand, is four times less than DenseNet201, InceptionResNetV2 which are 118 hidden layers as opposed to 402, 449 of DenseNet201 and InceptionResNetV2, separately. Although, the MobileNetV3Larege only achieve the accuracy of 0.86 the time need for prediction is 10 and 30 times less than the other opponents. If the MobileNetV3Large need a harder process of parameter hyper-tuning to achieve a better result, which is also the future target of this research.

4. Conclusions

In this paper, my objective is to analyze the effect of metadata on the performance of model as well as identifying whether metadata can make the model less imbalanced or not. On the other hand, I also try to construct an optimized and balanced model that can be used on mobile phone or electronic devices. The experiment shown that metadata improve the model performance, the factor that make the model much more imbalanced is the augmented data. This problem can be solve quite absolutely by using aforementioned weighted loss function. Using weighted loss function make the expected value of model

f1-score increase. At the end of the experiment, mobile model is found that can achieve 263
great performance without either the large number of parameters or depth. 264

Sample Availability: Samples of the compounds ... are available from the authors. 278

Abbreviations 279

The following abbreviations are used in this manuscript: 280

281

CAD	Computer aided diagnosis
AI	Artificial Intelligence
AKIEC	Actinic keratoses and intraepithelial carcinoma or Bowen's disease
BCC	Basal Cell Carcinoma
BKL	Benign Keratosis-like Lesions
DF	Dermatofibroma
MEL	Melanoma
NV	Melanocytic Nevi
VASC	Vascular Lesions
HISTO	Histopathology
FOLLOWUP	Follow-up examination
CONSENSUS	Expert Consensus
CONFOCAL	Confocal Microscopy
RGB	Red Green Blue
BGR	Blue Green Red
TP	True Positives
FN	False Negatives
TN	True Negatives
FP	False Positives
Sens	Sensitivity
Spec	Specificity
AUC	Area Under the Curve
ROC	Receiver Operating Curve

282

Appendix A Detailed Model Structure

DenseNet-201	DenseNet-201 + SA	Inception-ResNetV2	Inception-ResNetV2 + SA	ResNet-50	ResNet-50 + SA	ResNet-152	ResNet-152 + SA	NasNet-Large	NasNet-Large + SA
Conv2D 7x7	Conv2D 7x7	STEM	STEM	Conv2D 7x7	Conv2D 7x7	Conv2D 7x7	Conv2D 7x7	Conv2D 3x3	Conv2D 3x3
Pooling 3x3	Pooling 3x3			Pooling 3x3	Pooling 3x3	Pooling 3x3	Pooling 3x3	Pooling	Pooling
DenseBlock x 6	DenseBlock x 6	Inception ResNet A x 10	Inception ResNet A x 10	Residual Block x 3	Residual Block x 3	Residual Block x 3	Residual Block x 3	Reduction Cell x 2	Reduction Cell x 2
Conv2D 1x1	Conv2D 1x1	Reduction A	Reduction A					Normal Cell x N	Normal Cell x N
Average pool 2x2	Average pool 2x2								
DenseBlock x 12	DenseBlock x 12	Inception ResNet B x 20	Inception ResNet B x 20	Residual Block x 4	Residual Block x 4	Residual Block x 8	Residual Block x 8	Reduction Cell	Reduction Cell
Conv2D 1x1	Conv2D 1x1	Reduction B	Reduction B					Normal Cell x N	Normal Cell x N
Average pool 2x2	Average pool 2x2								
DenseBlock x 48	DenseBlock x 12	Inception ResNet C x 5	Inception ResNet C x 5	Residual Block x 6	Residual Block x 6	Residual Block x 36	Residual Block x 36	Reduction Cell	Reduction Cell
Conv2D 1x1	Conv2D 1x1							Normal Cell x N	Normal Cell x N-2
Average pool 2x2	Average pool 2x2								
DenseBlock x 29	DenseBlock x 29			Residual Block x 3		Residual Block x 3			
DenseBlock x 3	**SA Module**		**SA Module**		**SA Module**		**SA Module**		**SA Module**
GAP 7x7		Average pool		GAP 7x7		GAP 7x7			
FC 1000D		Dropout (0.8)		FC 1000D		FC 1000D			
SoftMax	SoftMax	SoftMax	SoftMax	SoftMax	SoftMax	SoftMax	SoftMax	SoftMax	SoftMax

Table A1. Details Structure of Models except Mobile models. SA stands for Soft-Attention, SA Module denotes whether that model use Soft-Attention Module. GAP stands for Global Average Pooling. FC stands for Fully-Connected Layer

Appendix B Detailed Mobile-based Model Structure

MobileNetV2	MobileNetV2 + SA	MobileNetV3 Small	MobileNetV3 Small + SA	MobileNetV3 Large	MobileNetV3 Large + SA	NasNet Mobile	NasNetMobile + SA
Conv2D	Conv2D	Conv2D 3x3	Conv2D 3x3	Conv2D 3x3	Conv2D 3x3	Normal Cell	Normal Cell
bottleneck	bottleneck	bottleneck 3x3 SE	bottleneck 3x3 SE	bottleneck 3x3 3 repeated	bottleneck 3x3 3 repeated	Reduction Cell	Reduction Cell
bottleneck 2 repeated	bottleneck 2 repeated	bottleneck 3x3	bottleneck 3x3	bottleneck 5x5 SE 3 repeated	bottleneck 5x5 SE 3 repeated	Normal Cell	Normal Cell
bottleneck 3 repeated	bottleneck 3 repeated	bottleneck 5x5 SE 8 repeated	bottleneck 5x5 SE 8 repeated	bottleneck 3x3 4 repeated	bottleneck 3x3 4 repeated	Reduction Cell	Reduction Cell
bottleneck 4 repeated	bottleneck 4 repeated			bottleneck 3x3 SE 2 repeated	bottleneck 3x3 SE 2 repeated	Normal Cell	
bottleneck 3 repeated	bottleneck 3 repeated			bottleneck 5x5 SE 3 repeated	bottleneck 5x5 SE 3 repeated		
bottleneck 3 repeated	bottleneck						
bottleneck							
Conv2D 1x1		Conv2D 1x1 SE	Conv2D 1x1 SE	Conv2D 1x1	Conv2D 1x1		
AP 7x7		Pool 7x7	Pool 7x7	Pool 7x7	Pool 7x7		
Conv2D 1x1	**SA Module**	Conv2D 1x1 2 repeated	**SA Module**	Conv2D 1x1 2 repeated	**SA Module**		**SA Module**
Softmax	Softmax	Softmax	Softmax	Softmax	Softmax	Softmax	Softmax

Table A2. Details Structure of Mobile based Models. SA stands for Soft-Attention, SA Module denotes whether that model use Soft-Attention Module. SE which stands for Squeeze-And-Excite shows whether that block has Squeeze-And-Excite.

Appendix C Detailed Model Performance

Appendix C.1 F1-Score Model Performance

Model	akiec	bcc	bkl	df	mel	nv	vasc	Mean
DenseNet201 with Augmented Data	0.56	0.75	0.64	0.62	0.60	0.93	0.85	0.70
InceptionResNetV2 with Augmented Data	0.42	0.63	0.51	0.35	0.57	0.9	0.7	0.58
Resnet50 with Augmented Data	0.39	0.59	0.42	0.6	0.42	0.88	0.79	0.58
VGG16 with Augmented Data	0.35	0.62	0.42	0.32	0.47	0.89	0.77	0.54
DenseNet201 with Metadata and WeightLoss	**0.84**	0.77	**0.81**	**0.83**	**0.69**	0.94	0.97	**0.83**
InceptionResNetV2 with Metadata and WeightLoss	0.77	0.83	**0.83**	0.64	**0.75**	0.94	0.7	**0.81**
Resnet50 with Metadata and WeightLoss	0.49	0.59	0.55	0.36	0.45	0.83	0.8	0.58
Resnet152 with Metadata and WeightLoss	0.42	0.38	0.41	0.15	0.4	0.75	0.75	0.46
NasNetLarge with Metadata and WeightLoss	0.79	0.79	0.8	0.74	0.65	0.92	0.92	**0.80**
MobileNetV2 with Metadata and WeightLoss	0.68	0.79	0.66	0.78	0.54	0.9	**0.9**	0.75
MobileNetV3Large with Metadata and WeightLoss	0.72	0.76	0.75	0.92	0.58	0.92	**0.92**	0.79
MobileNetV3Small with Metadata and WeightLoss	0.6	0.72	0.61	0.75	0.47	0.89	**0.89**	0.70
NasNetMobile with Metadata and WeightLoss	0.76	0.74	0.78	0.73	0.63	0.93	**0.93**	0.78

Table A3. F1-Score of each class: akiec, bcc, bkl, df, mel, nv, vasc which are denoted in the abbreviation. The last column is the expected value of f1-score from each model. All model in the first column is the models trained in this research. The term "with Augmented Data" means that model is trained with data augmenting during the training, there is no metadata or weight loss contribution. The term "with Metadata and WeightLoss" means that the model is trained with metadata including age, gender, localization and the weight loss function, there is no augmented data contribution

Appendix C.2 Recall Model Performance 287

Model	akiec	bcc	bkl	df	mel	nv	vasc	Mean
DenseNet201 with Augmented Data	0.65	0.75	0.59	0.53	0.54	0.93	0.85	0.69
InceptionResNetV2 with Augmented Data	0.37	0.60	0.55	0.24	0.59	0.9	0.67	0.56
Resnet50 with Augmented Data	0.33	0.56	0.38	0.53	0.40	0.92	0.81	0.56
VGG16 with Augmented Data	0.31	0.66	0.37	0.24	0.40	0.94	0.71	0.51
DenseNet201 with Metadata and WeightLoss	**0.85**	0.75	0.78	0.83	0.63	0.96	**1**	**0.82**
InceptionResNetV2 with Metadata and WeightLoss	**0.82**	0.84	0.81	0.67	0.7	0.95	0.93	**0.81**
Resnet50 with Metadata and WeightLoss	0.67	0.63	0.54	0.83	0.63	0.74	0.86	0.70
Resnet152 with Metadata and WeightLoss	0.51	0.49	0.35	0.76	0.47	0.63	0.48	0.52
NasNetLarge with Metadata and WeightLoss	0.73	0.71	**0.83**	**0.92**	0.59	0.9	0.93	**0.81**
MobileNetV2 with Metadata and WeightLoss	0.7	0.86	0.72	0.75	0.58	0.86	**1**	0.78
MobileNetV3Large with Metadata and WeightLoss	0.72	0.76	0.75	**0.92**	0.58	0.92	0.92	**0.80**
MobileNetV3Small with Metadata and WeightLoss	0.76	0.84	0.68	**1**	0.52	0.82	0.93	0.79
NasNetMobile with Metadata and WeightLoss	**0.82**	0.73	**0.83**	**0.92**	0.53	0.93	0.93	**0.81**

Table A4. Recall score of each class and the expected value of recall score from each model

Appendix C.3 Detailed Mobile Model Perform 288

Model	[21]	[22]Small	[22]Large	[33]Mobile
Accuracy(avg)	0.81	0.78	0.86	**0.86**
Balanced Accuracy(avg)	0.86	0.87	0.87	**0.88**
Precision(avg)	0.71	0.63	**0.75**	0.73
F1-score(avg)	0.75	0.70	**0.79**	0.78
Sensitivity(avg)	0.78	0.79	0.80	**0.81**
Specificity(avg)	0.95	0.95	0.95	**0.96**
ROC-AUC-score(avg)	0.96	0.95	0.96	**0.97**

Table A5. Deeper analyzing of mobile model. This table illustrate the other indicators of the four mobile-based models including MobileNetV2, MobileNetV3Small, MobileNetV3Large, NasNetMobile. The indicators are Accuracy, Balanced Accuracy, Precision, F1-score, Sensitivity, Specificity, and ROC - AUC score. All of them are average indicator

References

1. Katherine M. Li and Evelyn C. Li. Skin Lesion Analysis Towards Melanoma Detection via End-to-end Deep Learning of Convolutional Neural Networks. *Sensors* **2018**. 290 291
2. Xiaohan Xing and Yuenan Hou and Hang Li and Yixuan Yuan and Hongsheng Li and Max Q.-H. Meng Categorical Relation-Preserving Contrastive Knowledge Distillation for Medical Image Classification. *Springer Link* **2021**. 292 293
3. Rishu Garg and Saumil Maheshwari and Anupam Shukla Decision Support System for Detection and Classification of Skin Cancer using CNN. *Springer Link* **2019**. 294 295
4. Xuan Li and Yuchen Lu and Christian Desrosiers and Xue Liu Out-of-Distribution Detection for Skin Lesion Images with Deep Isolation Forest. *Springer Link* **2020**. 296 297

5. Amirreza Rezvantalab and Habib Safigholi and Somayeh Karimijeshni Dermatologist Level Dermoscopy Skin Cancer Classification Using Different Deep Learning Convolutional Neural Networks Algorithms. *Arxiv* **2021**.

6. Kyle Young and Gareth Booth and Becks Simpson and Reuben Dutton and Sally Shrapnel Dermatologist Level Dermoscopy Deep neural network or dermatologist?. *Nature* **2021**.

7. Philipp Tschandl and Cliff Rosendahl and Harald Kittler The HAM10000 data set, a large collection of multi-source dermatoscopic images of common pigmented skin lesions. *Nature* **2018**.

8. Michele Alberti and Angela Botros and Narayan Schuez and Rolf Ingold and Marcus Liwicki and Mathias Seuret Trainable Spectrally Initializable Matrix Transformations in Convolutional Neural Networks. *IEEE Xplore* **2019**.

9. Hemanth Nadipineni Method to Classify Skin Lesions using Dermoscopic images. *Arxiv* **2020**.

10. Nils Gessert and Maximilian Nielsen and Mohsin Shaikh and René Werner and Alexander Schlaefer Skin Lesion Classification Using Ensembles of Multi-Resolution EfficientNets with Meta Data. *Arxiv* **2020**.

11. Pranav Poduval and Hrushikesh Loya and Amit Sethi Functional Space Variational Inference for Uncertainty Estimation in Computer Aided Diagnosis. *Arxiv* **2020**.

12. Peng Yao and Shuwei Shen, Mengjuan Xu and Peng Liu and Fan Zhang and Jinyu Xing and Pengfei Shao and Benjamin Kaffenberger and Ronald X. Xu Single Model Deep Learning on Imbalanced Small Datasets for Skin Lesion Classification. *Arxiv* **2022**.

13. Manu Goyal and Thomas Knackstedt and Shaofeng Yan and Saeed Hassanpour Artificial Intelligence-Based Image Classification for Diagnosis of Skin Cancer: Challenges and Opportunities. *Arxiv* **2020**.

14. Soumyya Kanti Datta and Mohammad Abuzar Shaikh and Sargur N. Srihari and Mingchen Gao Soft-Attention Improves Skin Cancer Classification Performance. *SpringerLink* **2021**.

15. Amirreza Mahbod and Philipp Tschandl and Georg Langs and Rupert Ecker and Isabella Ellinger The Effects of Skin Lesion Segmentation on the Performance of Dermatoscopic Image Classification *Arxiv* **2020**.

16. Yeong Chan Lee and Sang-Hyuk Jung and Hong-Hee Won WonDerM: Skin Lesion Classification with Fine-tuned Neural Networks *Arxiv* **2019**.

17. Gao Huang and Zhuang Liu and Laurens van der Maaten and Kilian Q. Weinberger: Densely Connected Convolutional Network *IEEE Xplore* **2018**.

18. Mingxing Tan and Quoc V. Le EfficientNet: Rethinking Model Scaling for Convolutional Neural Networks *Arxiv* **2020**.

19. Christian Szegedy and Vincent Vanhoucke and Sergey Ioffe and Jonathon Shlens and Zbigniew Wojna Rethinking the Inception Architecture for Computer Vision *IEEE Xplore* **2015**.

20. Andrew G. Howard and Menglong Zhu and Bo Chen and Dmitry Kalenichenko and Weijun Wang and Tobias Weyand and Marco Andreetto and Hartwig Adam MobileNets: Efficient Convolutional Neural Networks for Mobile Vision Applications *Arxiv* **2017**.

21. Mark Sandler and Andrew Howard and Menglong Zhu and Andrey Zhmoginov and Liang-Chieh Chen MobileNetV2: Inverted Residuals and Linear Bottlenecks *IEEE Xplore* **2018**.

22. Andrew Howard and Mark Sandler and Grace Chu and Liang-Chieh Chen and Bo Chen and Mingxing Tan and Weijun Wang and Yukun Zhu and Ruoming Pang and Vijay Vasudevan and Quoc V. Le and Hartwig Adam Searching for MobileNetV3 *IEEE Xplore* **2019**.

23. Kaiming He and Xiangyu Zhang and Shaoqing Ren and Jian Sun Deep Residual Learning for Image Recognition *IEEE Xplore* **2015**.

24. Kaiming He and Xiangyu Zhang and Shaoqing Ren and Jian Sun Identity Mappings in Deep Residual Networks *Springer Link* **2016**.

25. Karen Simonyan and Andrew Zisserman Very Deep Convolutional Networks for Large-Scale Image Recognition *Arxiv* **2016**.

31. François Chollet Xception: Deep Learning with Depthwise Separable Convolutions *IEEE Xplore* **2017**.

27. Diederik P. Kingma, Jimmy Ba Adam: A Method for Stochastic Optimization *Arxiv* **2017**.

28. Kelvin Xu and Jimmy Ba and Ryan Kiros and Kyunghyun Cho and Aaron Courville and Ruslan Salakhutdinov and Richard Zemel and Yoshua Bengio Show, Attend and Tell: Neural Image Caption Generation with Visual Attention 2020 17th International Conference on Frontiers in Handwriting Recognition *PMLR* **2016**.

29. Mohammad Abuzar Shaikh and Tiehang Duan and Mihir Chauhan and Sargur N. Srihari. 2020 17th International Conference on Frontiers in Handwriting Recognition *IEEE Xplore* **2020**.

30. Naofumi Tomita and Behnaz Abdollahi and Jason Wei and Bing Ren and Arief Suriawinata and Saeed Hassanpour. Attention-Based Deep Neural Networks for Detection of Cancerous and Precancerous Esophagus Tissue on Histopathological Slides *Jama Network* **2020**.

31. Mohammad Abuzar Shaikh and Tiehang Duan and Mihir Chauhan and Sargur N. Srihari. 2020 17th International Conference on Frontiers in Handwriting Recognition *IEEE Xplore* **2019**.

32. Srihari. YAOSHIANG HO AND SAMUEL WOOKEY The Real-World-Weight Cross-Entropy Loss Function: Modeling the Costs of Mislabeling *IEEE Xplore* **2020**.

33. Barret Zoph, Vijay Vasudevan, Jonathon Shlens, Quoc V. Le Learning Transferable Architectures for Scalable Image Recognition *IEEE Xplore* **2017**.

34. Abien Fred Agarap Deep Learning using Rectified Linear Units (ReLU) *Arxiv* **2019**.

35. Jie Hu, Li Shen, Samuel Albanie, Gang Sun, Enhua Wu Squeeze-and-Excitation Networks *IEEE Xplore* **2019**.

36. Terrance DeVries, Graham W. Taylor Improved Regularization of Convolutional Neural Networks with Cutout *Arxiv* **2017**. 357
37. Christian Szegedy, Sergey Ioffe, Vincent Vanhoucke, Alex Alemi Inception-v4, Inception-ResNet and the Impact of Residual 358
    Connections on Learning *AAAI Conference* **2018**. 359